Lateral Vehicle Control Using Finite Spectrum Assignment ⋆

Illes Voros * **Balazs Varszegi** **

* *Department of Applied Mechanics, Budapest University of Technology and Economics*
** *Department of Applied Mechanics, Budapest University of Technology and Economics and MTA-BME Human Balancing Research Group (e-mail: varszegi@mm.bme.hu).*

Abstract: This paper investigates stability issues related to time delay in lateral vehicle control. First, the effects of feedback delay are examined in a single track vehicle model with proportional state feedback. The time delay is then compensated using a predictor based control approach called finite spectrum assignment (FSA). This controller calculates the states based on an internal model of the plant. This requires the online calculation of an integral term, which can negatively affect stability. The effects of parameter mismatches are also investigated. A comparison of delayed state feedback and the FSA controller is then carried out based on stability charts and numerical simulations. It is shown that the FSA has a significant advantage in performance compared to delayed state feedback even in the presence of parameter mismatches.

Keywords: Automotive control, autonomous vehicles, time delay, predictive control, finite spectrum assignment

1. INTRODUCTION

With the increasing number of driver assistance systems applied in today's automobiles and the continuous advances in autonomous driving, the importance of reliable stabilizing controllers is higher than ever. One very important aspect of such controllers is time delay: the presence of feedback delay in the control loop can cause oscillations and unstable behaviour. Delay compensation is therefore a highly important aspect of controller design.

Predictive controllers provide an efficient way of compensating time delay using an internal representation of the plant. Based on its internal model, the controller can estimate the current state of the process, thus the control action no longer needs to be generated according to the delayed information. The most widely known such controller is the Smith predictor (Smith (1957)). Since its introduction, several modifications of the Smith predictor have been published, including control methods such as the prediction based on optimal control (Kleinman (1969)), the reduction approach (Artstein (1982)), the predictive pole-placement control (Gawthrop (2002)) or the finite spectrum assignment (Manitius and Olbrot (1979); Wang et al. (1999)).

In vehicular technology, model predictive controllers based on optimizing a cost function are generally more widespread, both in path generating and path tracking (Ji et al. (2017); Schildbach and Borrelli (2015)). For an overview of motion planning techniques, please see González et al. (2016).

⋆ Supported by the ÚNKP-17-2-I New National Excellence Program of the Ministry of Human Capacities.

In this paper, a single track vehicle model is analyzed. First, the model is extended with delayed proportional state feedback in order to achieve stable rectilinear motion along a given line. This represents the simplest trajectory to follow, which allows us to reach compact, closed-form results. The analysis can be extended to more complex trajectories using the same principles. It is shown how the presence of feedback delay in the control loop negatively affects stable parameter domains. Next, the predictor based control method called finite spectrum assignment is applied to the vehicle model. This controller predicts the states by generating the solution of the system equations. This requires the online calculation of an integral term, which if done numerically, can result in unstable behaviour. The instability mechanisms related to numerical integration are analyzed in detail. Finally, a comparison of delayed state feedback and the FSA controller is presented using stability charts and numerical simulations. We pay particular attention to the effects of parameter mismatches.

The rest of this paper is organized as follows: the equations of the vehicle model are derived in Section 2. The application of delayed state feedback and the corresponding stability analysis is presented in Section 3. In Section 4, we introduce the FSA controller. This section is organized in three parts: first, the general concept of the controller is explained, then the instability mechanisms related to numerical quadrature are presented and finally the FSA controller is applied to the vehicle model. The effects of parameter mismatches and a comparison to delayed state feedback is presented in Section 5 using stability charts and numerical simulations. Finally, the results are concluded in Section 6.

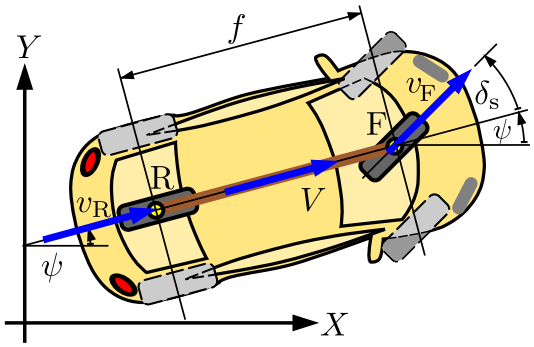

Fig. 1. The single track vehicle model.

2. MECHANICAL MODEL

The so-called single track (or bicycle) vehicle model is the most commonly used model to analyze lateral vehicle dynamics. We are going to investigate the in-plane motion of the single track model of a front wheel steered, rear wheel drive vehicle, with the assumption that no side slip occurs in the tire contact patch (see Fig. 1). This simplification keeps the equations of motion significantly less complicated, which in turn allows us to include exact, closed form expressions of the later analyses. On the other hand, only the kinematics of the vehicle are modeled this way.

The notations of the model are as follows: points F and R represent the front and rear axles respectively, the wheelbase is denoted by f and the steering angle is δ_s. The system states are the coordinates of point R x and y, and the vehicle heading ψ. The tires are not allowed to slip laterally, which means the direction of the wheels determine the direction of the corresponding velocity vectors. Furthermore, we fix the longitudinal velocity at a constant value V. The above simplifications can be expressed mathematically via the following kinematic constraints:

$$\begin{aligned} \dot{x}\sin(\psi+\delta_s) - \dot{y}\cos(\psi+\delta_s) - f\dot{\psi}\cos\delta_s &= 0\,, \\ -\dot{x}\sin\psi + \dot{y}\cos\psi &= 0\,, \\ \dot{x}\cos\psi + \dot{y}\sin\psi &= V\,. \end{aligned} \tag{1}$$

Solving the above system of equations for the derivatives of the states leads directly to the equations of motion of the vehicle:

$$\begin{aligned} \dot{x}(t) &= V\cos\psi(t)\,, \\ \dot{y}(t) &= V\sin\psi(t)\,, \\ \dot{\psi}(t) &= \tfrac{V}{f}\tan\delta_s(t)\,. \end{aligned} \tag{2}$$

3. STATE FEEDBACK

Our goal is to reach stable rectilinear motion along the $y = 0$ axis. This is going to be achieved by feeding back the states y and ψ, and generating the steering angle δ_s accordingly. With the introduction of control elements, however, feedback delay also appears in the system:

$$\delta_s(t-\tau) = -P_y y(t-\tau) - P_\psi\psi(t-\tau)\,, \tag{3}$$

where the delay term τ includes the feedback lag, the processing time of the controller and the dynamics of the steering mechanism. P_y and P_ψ represent the corresponding proportional gains.

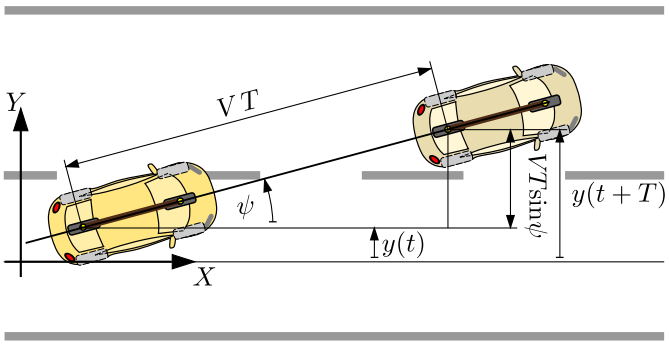

Fig. 2. Illustration of the preview control concept, where the desired trajectory is the middle of the lane.

Note that this control law can be considered as a linearized version of a proportional-derivative (PD) feedback controller, since

$$\delta_s(t) = -P_y y(t) - D_y\dot{y}(t) \approx -P_y y(t) - \underbrace{D_y V}_{=P_\psi}\psi(t) \tag{4}$$

using (2) and approximating $\sin\psi$ with ψ. Moreover, this is also identical to the basic preview model, where the vehicle lateral position T seconds ahead ($y(t+T)$) is used assuming a straight trajectory as it is shown in Fig. 2. The corresponding linearized control law in this case reads as

$$\delta_s(t) = -P_y y(t+T) \approx -P_y y(t) - \underbrace{P_y T V}_{=P_\psi}\psi(t)\,. \tag{5}$$

The linearized equations of motion can be written in the traditional state space form

$$\dot{\mathbf{x}}(t) = \mathbf{A}\mathbf{x}(t) + \mathbf{B}\mathbf{u}(t-\tau)\,. \tag{6}$$

Since the position along the x axis is not relevant in our case (it is a cyclic coordinate), it can be neglected, resulting in the state vector $\mathbf{x} = [y\ \ \psi]^{\mathrm{T}}$. The corresponding system matrix $\mathbf{A}$ and input matrix $\mathbf{B}$ are

$$\mathbf{A} = \begin{bmatrix} 0 & V \\ 0 & 0 \end{bmatrix}, \quad \mathbf{B} = \begin{bmatrix} 0 \\ V/f \end{bmatrix}. \tag{7}$$

The system input $\mathbf{u}(t)$ is the steering angle, which using the controller (3) can be written as

$$\mathbf{u}(t-\tau) = \mathbf{K}\mathbf{x}(t-\tau)\,, \tag{8}$$

where $\mathbf{K} = [-P_y\ -P_\psi]$ includes the control gains. This control method will be referred to as the PP controller. The characteristic equation of the system reads

$$\begin{aligned} D(\lambda) &= \det\left(\lambda\mathbf{I} - \mathbf{A} - \mathbf{B}\mathbf{K}e^{-\lambda\tau}\right) \\ &= \lambda^2 + \frac{P_\psi V e^{-\lambda\tau}}{f}\lambda + \frac{P_y V^2 e^{-\lambda\tau}}{f} = 0\,, \end{aligned} \tag{9}$$

where $\lambda = \sigma + j\omega$ is the characteristic exponent and $\mathbf{I}$ denotes the identity matrix. When there is no time delay present in the system ($\tau = 0$), the characteristic function $D(\lambda)$ reduces to a polynomial and the system's stability can be assessed using the Routh - Hurwitz criterion. In this case, assuming forward motion ($V > 0$), control parameters from the whole upper right quadrant of the $P_y - P_\psi$ plane result in stable behaviour.

When no feedback delay is present in the system, larger gains generally result in a faster response (as long as the resulting steering angle is lower than 90° - it is a simplification that the steering angle is not limited in our

model), but the presence of feedback delay severely limits the stable domains.

Static loss of stability occurs when a stable characteristic exponent crosses the imaginary axis in the origin. The condition $D(0) = 0$, considering that parameters f and V are not zero, translates into $P_y = 0$. On the boundary of dynamic stability loss (Hopf-bifurcation), the characteristic exponents are purely imaginary ($D(j\omega) = 0$). In this case, according to the D-subdivision method, the stability boundaries (or D-curves) can be determined by separating the real and imaginary parts of the characteristic equation and solving them for P_y and P_ψ:

$$P_y(\omega) = \frac{f\omega^2}{V^2}\cos(\omega\tau)\,, \qquad P_\psi(\omega) = \frac{f\omega}{V}\sin(\omega\tau)\,. \quad (10)$$

Here, ω represents the frequency of the resulting oscillatory motion at a given point of the stability boundary. Once the D-curves are known, the number of unstable characteristic exponents can be determined in each region using Stepan's formulae (see Stepan (1989)).

4. FINITE SPECTRUM ASSIGNMENT

In this section, we are going to introduce a predictive model based controller called finite spectrum assignment (FSA) (Manitius and Olbrot (1979); Wang et al. (1999); Jankovic (2009)). The main idea behind this control method is that a mathematical model that perfectly describes the dynamics of a system allows us to determine the states for any time instant given that an initial condition is known. In other words, the controller can compensate time delay by estimating the current states based on an internal model of the system and the delayed sensor information (see Fig. 3).

4.1 General concept

If the system to be controlled is of the form (6), the internal model of the controller is

$$\dot{\mathbf{x}}(t) = \widetilde{\mathbf{A}}\mathbf{x}(t) + \widetilde{\mathbf{B}}\mathbf{u}(t-\tilde{\tau})\,, \quad (11)$$

where the tildes denote the model parameters used within the controller. In order to compensate the time delay τ of the real system, the control signal has to be in the form $\mathbf{u}(t-\tau) = \mathbf{K}\mathbf{x}(t)$, which means that despite the time delay, the controller has to act based on the current system states. This is equivalent to $\mathbf{u}(t) = \mathbf{K}\mathbf{x}(t+\tau)$, which shows that the required system states are in the future from the controller's point of view. These future states are estimated by taking the solution of (11) with the initial condition $\mathbf{x}(t-\tilde{\tau})$ over the time interval $\tilde{\tau}$. This results in the control signal

$$\mathbf{u}(t) = \mathbf{K}e^{\widetilde{\mathbf{A}}\tilde{\tau}}\mathbf{x}(t) + \mathbf{K}\int_{-\tilde{\tau}}^{0} e^{-\widetilde{\mathbf{A}}s}\widetilde{\mathbf{B}}\mathbf{u}(t+s)\mathrm{d}s\,. \quad (12)$$

The above formula shows that the control signal in any given time is based on the latest available state feedback and the past control actions generated over the delay period. If the internal model perfectly describes the dynamics of the real system and all the parameters are exactly known, then the delay terms cancel out and the system can be simplified to the form $\dot{\mathbf{x}}(t) = (\mathbf{A}+\mathbf{B}\mathbf{K})\,\mathbf{x}(t)$. This, however, assumes a perfect implementation of the control law, which in most cases is impossible to achieve in practice.

4.2 Implementation

Using numerical quadrature to approximate the integral term of (12) results in

$$\mathbf{u}(t) = \mathbf{K}e^{\widetilde{\mathbf{A}}\tilde{\tau}}\mathbf{x}(t) + \mathbf{K}\sum_{j=0}^{\tilde{r}} e^{\widetilde{\mathbf{A}}\theta_{j,\tilde{r}}}\widetilde{\mathbf{B}}\mathbf{u}(t-\theta_{j,\tilde{r}})h_{j,\tilde{r}}\,, \quad (13)$$

where $\theta_{j,\tilde{r}} \in [0,\tilde{\tau}]$, $h_{j,\tilde{r}} \in \mathbb{R}$, and $\tilde{r}$ is an integer that determines the precision of the approximation: $\tilde{r} \to \infty$ produces the exact value of the integral.

The numerical approximation replaces the distributed time delay in (12) with a sum of point delays. This leads to a set of neutral functional differential equations:

$$\dot{\mathbf{x}}(t) = \mathbf{A}\mathbf{x}(t) + \mathbf{B}\mathbf{u}(t-\tau)\,, \quad (14)$$

$$\begin{aligned}\dot{\mathbf{u}}(t) = {} & \mathbf{K}e^{\widetilde{\mathbf{A}}\tilde{\tau}}\mathbf{A}\mathbf{x}(t) + \mathbf{K}e^{\widetilde{\mathbf{A}}\tilde{\tau}}\mathbf{B}\mathbf{u}(t-\tau) + \\ & + \sum_{j=0}^{\tilde{r}} \mathbf{K}e^{\widetilde{\mathbf{A}}\theta_{j,\tilde{r}}}\widetilde{\mathbf{B}}\dot{\mathbf{u}}(t-\theta_{j,\tilde{r}})h_{j,\tilde{r}}\,.\end{aligned} \quad (15)$$

However, the above system can become unstable for arbitrarily large values of $\tilde{r}$ even when the original system is stable (Michiels and Niculescu (2007)). The reason for this is the appearance of unstable characteristic roots with a large absolute value when using numerical quadrature. As $\tilde{r}$ is increased, some of these poles tend to those of the original system, while others may converge to infinity without leaving the right half plane.

A necessary condition for the stability of the system (6) and (13) for sufficiently large values of $\tilde{r}$ (assuming that the original system defined by (6) and (12) is stable) is the stability of the difference equation

$$\mathbf{u}(t) = \sum_{j=0}^{\tilde{r}} \mathbf{K}e^{\widetilde{\mathbf{A}}\theta_{j,\tilde{r}}}\widetilde{\mathbf{B}}\mathbf{u}(t-\theta_{j,\tilde{r}})h_{j,\tilde{r}}\,. \quad (16)$$

If $\tilde{r} \to \infty$, the roots of equation (16) tend to the roots of the functional difference equation

$$\mathbf{u}(t) = \mathbf{K}\int_{-\tilde{\tau}}^{0} e^{-\widetilde{\mathbf{A}}s}\widetilde{\mathbf{B}}\mathbf{u}(t+s)\mathrm{d}s\,. \quad (17)$$

Following Michiels et al. (2003) and Molnar and Insperger (2016), we are going to refer to the stability of the original system as *ideal stability* and to the stability of (17) as *theoretical stability*. Meeting both conditions ensures that all poles of the system with the numerical integration are on the left half plane. However, the system might still become unstable because of arbitrarily small perturbations of the discretization parameter $\theta_{j,\tilde{r}}$. This may occur during practical application or with the use of specific integration schemes. In order to ensure *robust stability* with regards to perturbations of $\theta_{j,\tilde{r}}$, the strong stability of the delay-difference equation (16) is required. The necessary and sufficient condition for this (see Michiels et al. (2003)) in the single input case is

$$S = \int_0^{\tilde{\tau}} \left|\mathbf{K}e^{\widetilde{\mathbf{A}}s}\widetilde{\mathbf{B}}\right| \mathrm{d}s < 1\,. \quad (18)$$

The conditions of theoretical and robust stability, however, are related to high frequency ranges. Therefore the corresponding restrictions can be avoided with the application of a low-pass filter or a digital controller. For example,

an implementation using dynamic feedback is presented in Mondie and Michiels (2003), which results in a low-pass filtering behaviour of the control law. For further alternatives, the reader is referred to Zhong (2006).

4.3 Application on the vehicle model

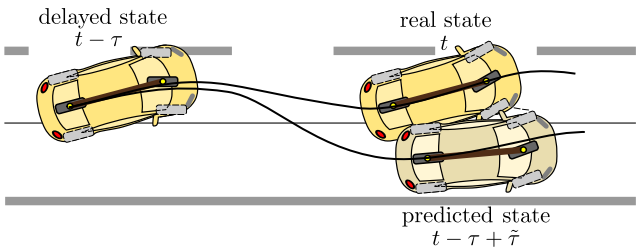

Fig. 3. Illustration of the prediction concept, where the desired trajectory is the middle of the lane.

We are going to include the single track vehicle model as the internal model (11) of the FSA controller, with the notations

$$\widetilde{\mathbf{A}} = \begin{bmatrix} 0 & \tilde{V} \\ 0 & 0 \end{bmatrix}, \quad \widetilde{\mathbf{B}} = \begin{bmatrix} 0 \\ \tilde{V}/\tilde{f} \end{bmatrix}. \tag{19}$$

This way, following (12), the steering angle is defined as

$$\begin{aligned} \delta_{\mathrm{s}}(t) = [-P_y \ -P_\psi] \Bigg(\begin{bmatrix} 1 & \tilde{V}\tilde{\tau} \\ 0 & 1 \end{bmatrix} \begin{bmatrix} y(t) \\ \psi(t) \end{bmatrix} \\ + \int_{-\tilde{\tau}}^{0} \begin{bmatrix} 1 & -s\tilde{V} \\ 0 & 1 \end{bmatrix} \begin{bmatrix} 0 \\ \tilde{V}/\tilde{f} \end{bmatrix} \delta_{\mathrm{s}}(t+s)\mathrm{d}s \Bigg) . \end{aligned} \tag{20}$$

Using the exponential trial function $\mathbf{C}e^{\lambda t}$ ($\mathbf{C} \in \mathbb{C}^3$), the linearized vehicle model with the steering angle (20) can be written in the matrix form

$$\underbrace{\begin{bmatrix} \lambda & -V & 0 \\ 0 & \lambda & \frac{V}{f}e^{-\lambda\tau} \\ P_y & P_\psi + P_y\tilde{V}\tilde{\tau} & g(\lambda) \end{bmatrix}}_{\mathbf{M}(\lambda)} \mathbf{C} = \mathbf{0}, \tag{21}$$

where

$$\begin{aligned} g(\lambda) = \frac{1}{\tilde{f}\lambda^2} \Big(\tilde{f}\lambda^2 - \tilde{V}e^{-\lambda\tilde{\tau}} \Big(P_y(\lambda\tilde{\tau}\tilde{V} + \tilde{V}) + \lambda P_\psi \Big) \\ + P_y\tilde{V}^2 + \lambda P_\psi \tilde{V} \Big) . \end{aligned} \tag{22}$$

The characteristic equation of the system is

$$D(\lambda) = \det \mathbf{M}(\lambda) = 0, \tag{23}$$

which is used to assess ideal stability.

Theoretical stability depends on the characteristic equation of (17), which in our case can be reached by substituting $\mathbf{x}(t) \equiv \mathbf{0}$ and $\delta_{\mathrm{s}}(t) = \delta_{\mathrm{s},0}\, e^{\lambda t}$ into the control law:

$$\begin{aligned} D(\lambda) = \frac{1}{\tilde{f}\lambda^2} \Big(\Big(\lambda(\tilde{f}\lambda + P_\psi\tilde{V}) + P_y\tilde{V}^2 \Big) + \\ - e^{-\lambda\tilde{\tau}}\tilde{V} \Big(P_y(\lambda\tilde{\tau}\tilde{V} + \tilde{V}) + \lambda P_\psi \Big) \Big) . \end{aligned} \tag{24}$$

Finally, robust stability with respect to the integral time step is ensured if the following holds:

$$S = \int_0^{\tilde{\tau}} \left| \frac{\tilde{V}(-P_y s\tilde{V} - P_\psi)}{\tilde{f}} \right| \mathrm{d}s < 1 . \tag{25}$$

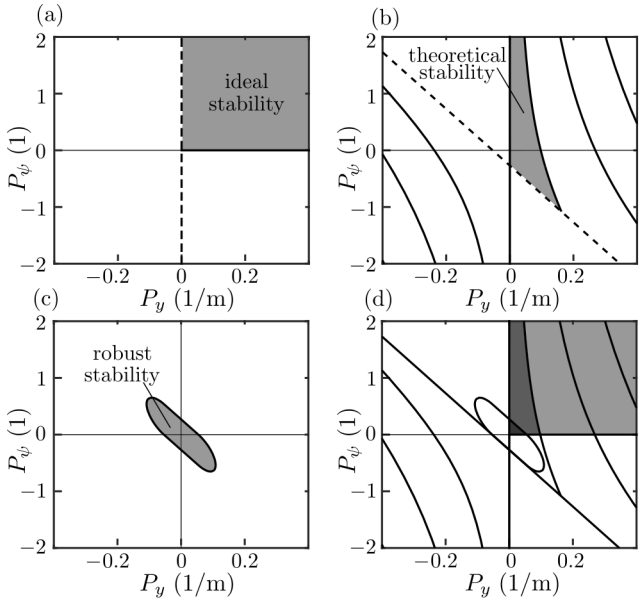

Fig. 4. Stability charts of the FSA controller applied to the single track vehicle model with no parameter mismatches: (a) the region of ideal stability, (b) stability of the associated functional difference equation (required to achieve theoretical stability), (c) stability of the associated delay-difference equation (required for robust stability), and (d) their superposition (f = 2.7 m, V = 20 m/s, τ = 0.5 s).

If the internal model of the FSA controller is a perfect representation of the real system ($\widetilde{\mathbf{A}} = \mathbf{A}$ and $\widetilde{\mathbf{B}} = \mathbf{B}$), then the characteristic equation (23) reduces to the characteristic equation (9) of normal state feedback with no time delay ($\tau = 0$). This means that in this case the conditions of ideal stability are the same as the stability conditions of the delay free system, and the corresponding stability maps are identical. The conditions of theoretical and robust stability, however, cannot be further simplified in case of a perfect internal model, because these depend only on the controller and not the real system.

The stability charts of ideal, theoretical and robust stability of the FSA controller can be seen in Fig. 4. Control gains that are not within the region of ideal stability (Fig. 4 (a)) result in unstable behaviour. Parameter pairs that are in this region but are not theoretically stable (Fig. 4 (b)) may become unstable when applying numerical integration. Finally, robust stability with regards to the integration time step can only be guaranteed in the region where the condition (25) is also met (Fig. 4 (c)). This means that considering all the effects related to numerical integration reduces the stable area to the intersection of the previous 3 regions (Fig. 4 (d)). Alternatively, as we mentioned previously, the restrictions of theoretical and robust stability can be avoided by applying a low-pass filter or a digital controller.

Fig. 5 illustrates the system response related to the above instability mechanisms. The simulation time step was set to 0.005 s, while the integration within the FSA controller was performed using rectangular approximation with a periodically varied time step of Δt_1 = 0.05 s, $\Delta t_2 = 1.5\Delta t_1$, $\Delta t_3 = \Delta t_1$ and $\Delta t_4 = 0.5\Delta t_1$. Because of this variation of

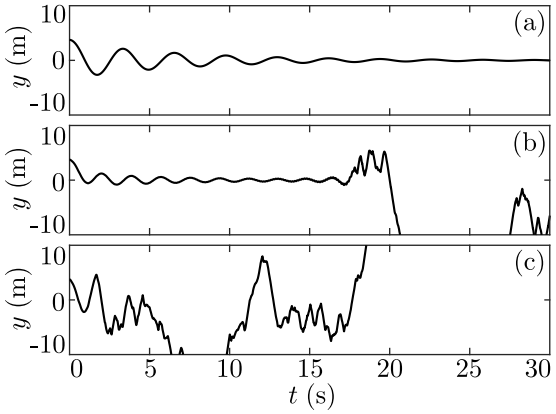

Fig. 5. System response of the vehicle model with FSA using a rectangular approximation of the integral with periodically varied time steps. The control parameters are chosen such that (a) robust stability is ensured, (b) the system is theoretically stable, but not robustly stable, (c) only ideal stability is ensured ($f = 2.7$ m, $V = 20$ m/s, $\tau = 0.5$ s).

the integration time step, the system can only be stabilized by control parameters from the robustly stable domain. The corresponding system response is shown in Fig. 5 (a). When the chosen control parameters are outside the robustly stable area but they are still theoretically stable, the resulting system response is unstable (Fig. 5 (b)). Using a uniform integration time step, however, would result in stable behaviour. In case (c), we used control parameters that are outside the theoretically stable domain but they are still ideally stable. In this case, the simulation can only be stabilized by setting an equal (constant) simulation and integration time step, which would correspond to a discretized approximation of a system that uses a continuous implementation of the integral.

5. STABILITY CHARTS, NUMERICAL SIMULATIONS

In this section, we are going to compare the performance of the two controllers, as well as analyze the sensitivity of the FSA controller to parameter mismatches. Parameter mismatches of the internal model of the controller degrade performance and can even cause stability loss. Fig. 6 shows the regions of ideal stability of the FSA controller with varying degrees of parameter mismatches in terms of velocity V and time delay τ. The third parameter, the vehicle wheelbase f, is assumed to be known precisely. Although the stable region of the PP controller remains the same in all 9 cases, it is shown for comparison purposes. Assuming a digital implementation, the regions of theoretical and robust stability are not included in this comparison.

According to the charts of Fig. 6, the stable regions of the FSA controller are considerably larger than simple state feedback, even when the internal model parameters are 20% inaccurate. It's also apparent that the stable areas are much more sensitive to the accuracy of time delay than to the accuracy of velocity. The larger stable domains allow for higher gains, which lead to a faster system response.

Numerical simulations were also performed based on the 9 cases of Fig. 6, using the nonlinear vehicle model (see

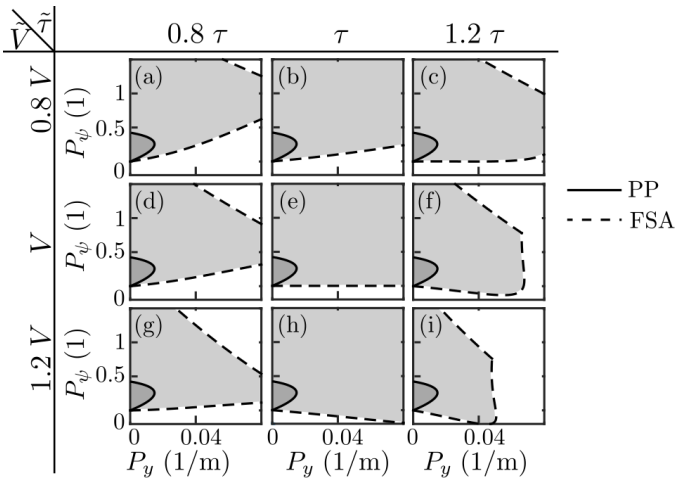

Fig. 6. Stable regions of the PP controller and the FSA controller in case of −20%, 0% and +20% errors in the estimated vehicle velocity and time delay ($f = 2.7$ m, $V = 20$ m/s, $\tau = 0.5$ s).

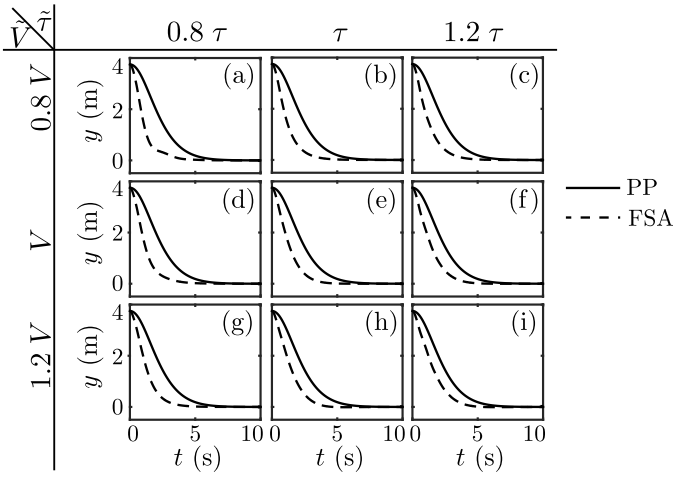

Fig. 7. Simulation results of the PP controller and the FSA controller in case of −20%, 0% and +20% errors in the estimated vehicle velocity and time delay ($f = 2.7$ m, $V = 20$ m/s, $\tau = 0.5$ s).

Fig. 7). The initial position was set to $y(0) = 3.75$ m, the simulation time step was 0.001 s, and the integration time step of the FSA controller was set to 0.05 s. The control parameters were determined using the semi-discretization method (Insperger and Stepan (2011)): after numerically evaluating the stable domains point by point, we chose the parameter pairs where the characteristic multipliers of the semi-discrete system had the smallest modulus. This results in the most highly damped system response. In case of state feedback these optimal values are $P_y = 0.0022$ 1/m, $P_\psi = 0.1250$, and for the FSA controller (with perfect internal model) $P_y = 0.0165$ 1/m and $P_\psi = 0.4239$. The lateral vehicle positions are presented in Fig. 7, while the numerical values of settling time are listed in Table 1 (we define settling time as the lowest time instant t_0 where $|y(t)| < 0.02\,|y(0)|$ for $\forall t > t_0$).

Because of no modeling errors and an accurate enough implementation of the integral, the FSA controller almost completely removes the time delay in case (e), which means

Table 1. Settling Time Values of the Numerical Simulations in Seconds

Case	PP	FSA
(a)	6.428	4.324
(b)	6.428	4.265
(c)	6.428	4.593
(d)	6.428	4.377
(e)	6.428	4.188
(f)	6.428	4.645
(g)	6.428	4.25
(h)	6.428	4.234
(i)	6.428	4.776

that its system response in that case is practically the same as the response of the delay free PP controller. In all the other cases, the parameter mismatches degrade the performance of the FSA, although it is still much faster than simple state feedback, thanks to the larger gains. As the stability charts have already suggested, inaccuracies in the estimated time delay cause the biggest decline in performance. The 3 worst cases are (c), (f) and (i), where the feedback delay is consistently overestimated. We experience the longest settling time in case (i), where both the time delay and the velocity terms have an error of +20%, which results in the largest overestimation of the distance covered during the delay interval.

It is worth noting that for the sake of more notable differences in the simulations, we used a conservative estimate for the feedback delay. In practice, depending on the details of the implementation and the design goals, the feedback delay can be expected to be lower than 500 ms, which leads to larger stable domains, higher permissible gains and thus faster responses.

6. CONCLUSIONS

A single track vehicle model with feedback delay was analyzed in this paper. First, we applied proportional state feedback and presented how time delay affects the stable parameter domains. Then the predictive control method called finite spectrum assignment was introduced to compensate deadtime. Stability issues related to implementation difficulties and parameter mismatches were discussed. We compared the performance of the FSA controller with delayed state feedback using stability charts and numerical simulations. The FSA significantly outperformed state feedback even when the system parameters had an error of 20%.

A very simple vehicle model was used in this comparison, so that the fundamentals of the controllers could be presented in a compact, easy to understand form. In practice, however, there will always be differences not only between the parameters, but between the dynamics of the internal model and the controlled system too. Therefore, as far as computational resources allow it, a more detailed internal model is recommended to use.

REFERENCES

Artstein, Z. (1982). Linear systems with delayed controls: A reduction. *IEEE Transactions on Automatic Control*, 27(4), 869–879.

Gawthrop, P.J. (2002). Predictive pole-placement control with linear models. *Automatica*, 38(3), 421–432.

González, D., Pérez, J., Milanés, V., and Nashashibi, F. (2016). A review of motion planning techniques for automated vehicles. *IEEE Transactions on Intelligent Transportation Systems*, 17(4), 1135–1145.

Insperger, T. and Stepan, G. (2011). *Semi-Discretization for Time-Delay Systems*. Springer.

Jankovic, M. (2009). Forwarding, backstepping, and finite spectrum assignment for time delay systems. *Automatica*, 45(1), 2–9.

Ji, J., Khajepour, A., Melek, W.W., and Huang, y. (2017). Path planning and tracking for vehicle collision avoidance based on model predictive control with multiconstraints. *IEEE Transactions on Vehicular Technology*, 66(2), 952–964.

Kleinman, D. (1969). Optimal control of linear systems with time-delay and observation noise. *IEEE Transactions on Automatic Control*, 14(5), 524–527.

Manitius, A.Z. and Olbrot, A.W. (1979). Finite spectrum assignment problem for systems with delays. *IEEE Transactions on Automatic Control*, 24(4), 541–553.

Michiels, W., Mondie, S., and Roose, D. (2003). Robust stabilization of time-delay systems with distributed delay control laws: Necessary and sufficient conditions for a safe implementation. Technical report, Katholieke Universiteit Leuven, Belgium.

Michiels, W. and Niculescu, S.I. (2007). *Stability and Stabilization of Time-Delay Systems*. Society for Industrial & Applied Mathematics, U.S.

Molnar, T. and Insperger, T. (2016). On the robust stabilizability of unstable systems with feedback delay by finite spectrum assignment. *Journal of Vibration and Control*, 22(3), 649–661.

Mondie, S. and Michiels, W. (2003). Finite spectrum assignment of unstable time-delay systems with a safe implementation. *IEEE Transactions on Automatic Control*, 48(12), 2207–2212.

Schildbach, G. and Borrelli, F. (2015). Scenario model predictive control for lane change assistance on highways. In *IEEE Intelligent Vehicles Symposium (IV)*. IEEE.

Smith, O.J. (1957). Closer control of loops with dead time. *Chemical Engineering Progress*, 53(5), 217–219.

Stepan, G. (1989). *Retarded Dynamical Systems: Stability and Characteristic Functions*. Longman Scientific & Technical.

Wang, Q.G., Tong, H.L., and Kok, K.T. (1999). *Finite-Spectrum Assignment for Time-Delay Systems*. Springer-Verlag London.

Zhong, Q.C. (2006). *Robust Control of Time-delay Systems*. Springer-Verlag London.